ELSEVIER

Ceramics International 25 (1999) 309–315

CERAMICS INTERNATIONAL

Wear behavior of Si_3N_4 ceramic cutting tool material against stainless steel in dry and water-lubricated conditions

Zhao Xingzhong, Liu Jiajun*, Zhu Baoliang, Miao Hezhou, Luo Zhenbi

Tribology Research Institute, Tsinghua University, Beijing 100084, People's Republic of China

Received 21 April 1997; accepted 10 January 1998

Abstract

Si_3N_4-based ceramic cutting tools have been used successfully for machining hard materials, like: cast irons, nickel based alloys etc. Austenitic stainless steel AISI 321 is one of the most difficult-to-cut materials. In order to investigate the wear behavior of Si_3N_4 ceramic when cutting the stainless steel the wear tests were carried out on a pin-on-disk tribometer, which can simulate a realistic cutting process. The selected load range was from 58.8 N to 235.2 N, the speed range was from 0.8 m/s to 3.2 m/s. The experiment results showed that the wear of Si_3N_4 ceramic increases with both load and speed. In dry conditions, the wear of ceramic is mainly caused by adhesion between the rubbing surfaces. In water-lubricated conditions, microfracture of the ceramic may be increased due to stress corrosion of water to the ceramic surface, in addition, the wear is also attributed to adhesion and chemical action of water with the Si_3N_4 surface. Scanning electron microscopy (SEM), electron probe microanalyzer (EPMA), Auger electron spectroscopy (AES) and energy dispersive X-ray analyzer (EDX) were used for examining of the worn surfaces. The wear mechanisms of Si_3N_4 ceramic sliding against the stainless steel were discussed in detail. © 1999 Published by Elsevier Science Limited and Techna S.r.l. All rights reserved.

Keywords: D. Silicon nitride; Stainless steel; Adhesive wear; Tribochemistry

1. Introduction

During the last 20 years, Si_3N_4-based ceramics have been increasingly used as wear resistant materials. One of the most important applications of these materials is making cutting tools, which are applied successfully in machining cast irons and nickel-based alloys [1–4], However, their performance for cutting steels is less than satisfactory [5]. The wear rate of a silicon nitride cutting tool is two orders of magnitude higher when machining AISI 1045 steel than machining grey cast iron [6]. The high cratering wear of sialon ceramic when machining AISI 1045 steel is caused by the chemical dissolution of sialon grains, followed by pull out of sialon grains from the glassy intergranular phase [7].

Austenitic stainless steels is a commonly used corrosion-resistant metallic material. However, a little knowledge about the wear behavior of Si_3N_4 based ceramics against austenitic stainless steel is available. The objective of this study is to investigate the wear behavior of a Si_3N_4-based ceramic against stainless steel on a pin-on-disk tribometer under dry and water-lubricated conditions. Comparing with real machining test, the pin-on-disk tests are simple, quick and the test conditions may be widely varied and well controlled. Some works about wear mechanism analysis of ceramic tool materials and the comparison of wear data for pin-on-disk tests and cutting behavior of ceramics have been published, some correlation has been found between the wear resistance of tool materials on a pin-on-disk machine and the life of cutting tools [8,9]. In this research, the worn surfaces of Si_3N_4 ceramic were examined and analyzed by using scanning electron microscopy (SEM), electron probe microanalyzer (EPMA), Auger electron spectroscopy (AES) and energy dispersive X-ray analyzer (EDX).

2. Experimental procedure

2.1. Test machine and specimens

Wear tests were carried out on a pin-on-disk tribometer. The pin specimen was fixed, the disk specimen

* Corresponding author.

0272-8842/99/$20.00 © 1999 Published by Elsevier Science Limited and Techna S.r.l. All rights reserved.
PII: S0272-8842(98)00040-6

rotated at different speeds. The contact model of pin and disc, and the wear scar of the pin is shown in Fig. 1. The line contact can simulate well the contact form of cutting tool and workpiece in a realistic cutting practice. The pin specimen was made from hot pressed Si_3N_4 ceramic, having a size of 5×5×25 mm; and the disk was machined from AISI 321 stainless steel with 56 mm in diameter and 6 mm in thickness. The surface roughnesses of pin and disk were Ra = 0.32 μm and Ra = 0.21 μm respectively. The composition and properties of the Si_3N_4 ceramic are listed in Table 1.

2.2. Experimental Method

Friction and wear tests were conducted under dry and water-lubricated conditions. The distilled water was fed into the contact zone by drop flow. The average rate of flow was about 0.015 l/min. The sliding speeds were varied from 0.8 m/s to 3.2 m/s, and the load range was from 58.8 N to 235.2 N. Each new pair had a 30 min running time under selected speed and load, and each test was repeated 2–3 times. Before and after testing, the specimens were ultrasonically cleaned in acetone bath for 15 min.

The wear scar width of the pin was measured under a light microscope, then the volume and wear rate could be calculated. The friction force is transmitted by a transducer to a recorder continuously during the test, from which the friction coefficient could be obtained. The worn surfaces were analysed by SEM, EDX, EPMA and X-ray diffraction spectroscopy (XRD).

Table 1
The composition and properties of the Si_3N_4 ceramic

Composition	Si_3N_4(>80%),TiC,Al_2O_3
Density (g/cm^3)	3.5
Hardness (Hv)	1900
Bending strength (MPa)	750
Elastic modulus (GPa)	290
Fracture toughness (MPa m$^{1/2}$)	6.3
Grain size (μm)	<1.3

3. Results and discussion

3.1. Effect of load on friction and wear

Figs. 2 and 3 show the variation of friction coefficient and wear rate with load, respectively. It can be seen that the friction coefficient and wear rate of the ceramic increase with load under both dry and lubricated conditions. In dry condition, the stainless steel can adhere on the ceramic surface at both low and high loads. The rapid increase of the wear rate under dry conditions at higher load (235.2 N) may be caused by the severe adhesion and the adhesion-induced microfracture of the ceramic, which was confirmed by the SEM examinations of the worn Si_3N_4 ceramic surface, see Fig. 4 (the arrow in Fig. 4 indicates the microfracture pit) and Fig. 5 (SEM morphology of Si_3N_4 surface at lower load).

3.2. Effect of sliding speed on friction and wear

The variations of friction coefficient and wear rate with speed are shown in Figs. 6 and 7. Similar to the effect of load, the friction coefficient and wear rate increase with speed, under dry conditions, however, the friction coefficient increases more rapidly and reaches a much higher value compared with the effect of load. High speed brings about large amounts of friction heat, which will cause more severe adhesion of the rubbing surfaces, and in consequence, increase the friction coefficient and wear rate. In general, the effect of sliding speed is more obvious than load in producing the friction heat. The SEM morphologies of the worn Si_3N_4 surfaces obtained at different speeds are similar to Figs. 4 and 5.

3.3. Wear mechanisms of Si_3N_4 ceramic under dry conditions

In order to reveal the wear mechanism of Si_3N_4 ceramic, the SEM was employed to examine the worn surfaces. From the observations (Figs. 4 and 5), it is not difficult to deduce the wear process of the Si_3N_4 ceramic

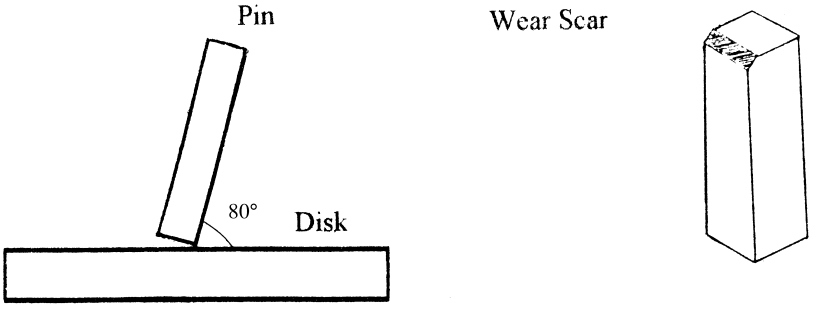

Fig. 1. The contact model of the pin and the disk.

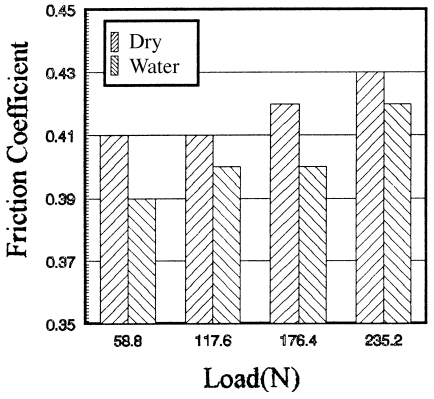

Fig. 2. Variation of friction coefficient with load.

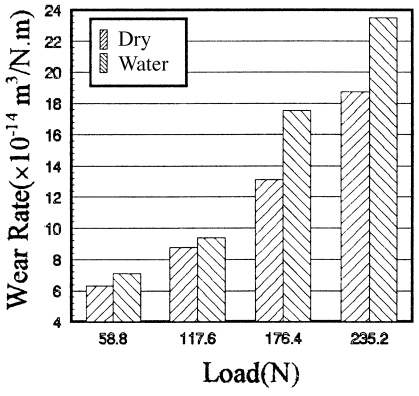

Fig. 3. Variation of wear rate of the ceramic with load.

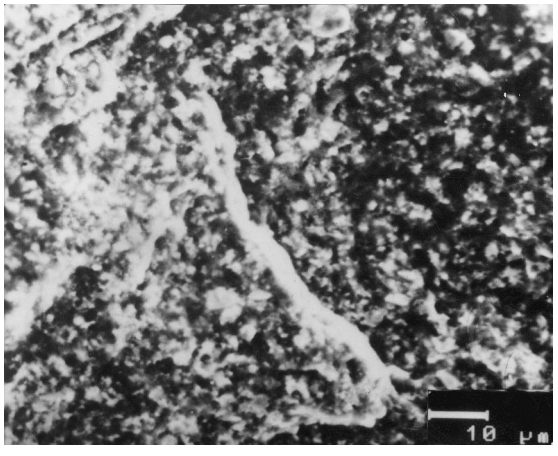

Fig. 4. SEM morphologies of the worn ceramic surfaces (dry, 235.2 N, 1.6 m/s).

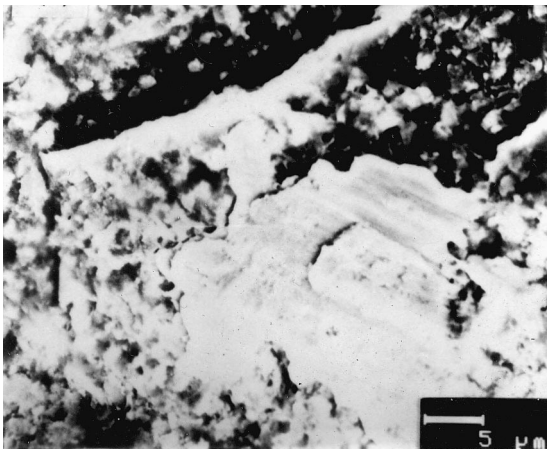

Fig. 5. SEM morphology of the worn ceramic (dry, 117.6 N, 1.6 m/s).

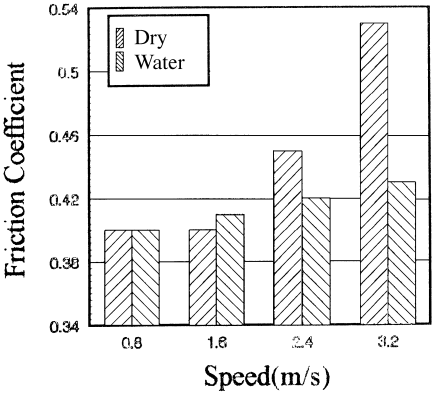

Fig. 6. Variation of friction coefficient with speed.

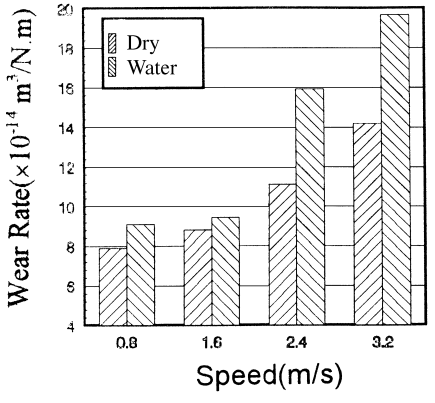

Fig. 7. Variation of wear rate of the ceramic with speed.

as follows: Due to the high chemical affinity between iron and silicon nitride [10,11], a strong adhesion will occur when Si_3N_4 is sliding against stainless steel. The adhesion spots will be torn off with the relative movement of the rubbing surfaces, resulting in the transfer of stainless steel on the ceramic surface because the former has relatively low shear strength.

The ceramic surface with transferred stainless steel is always subjected to the shear and compressive stresses repeatedly in the sliding process, which will cause the formation of microcracks and microfractures on the ceramic surface or its subsurface. Meanwhile, the transferred stainless steel layer is also subjected to the adhesive force coming from the counterpart of stainless steel

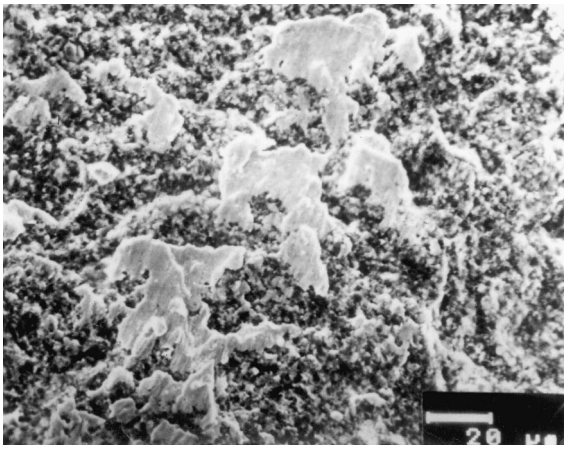

Fig. 8. SEM morphology of the worn ceramic surface (dry friction, 235.2 N, 1.6 m/s).

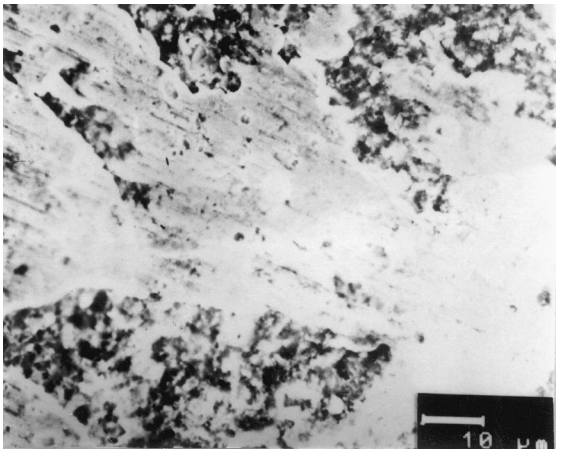

Fig. 10. SEM morphology of the worn ceramic surface (water-lubricated, 117.6 N, 1.6 m/s).

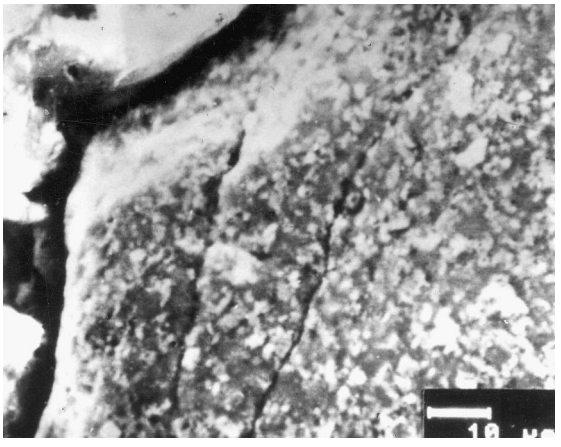

Fig. 9. SEM examination on the transverse section of the worn ceramic surface (dry friction, 235.2 N, 1.6 m/s).

which can peel off the transferred stainless steel layer. Some ceramic microfracture pieces or Si_3N_4 grains will also be peeled off or pull out and quit the ceramic surface with the peeled off stainless steel layer, which gives rise to the wear of the ceramic.

The adhesion-peeling off mechanism of the ceramic wear can be confirmed by the SEM examinations of the worn ceramic surface and its transverse section, see Figs. 8 and 9. Microcracks were formed in both the worn ceramic surface and its subsurface.

3.4. Influence of water on friction and wear

Comparing with dry frictional conditions, the friction coefficient decreased a little and the wear rate increased in water-lubricated conditions, see Figs. 2 and 3. The amount of the transferred stainless steel was reduced due to the existence of water, see Fig. 10. However, the lubricity of water is rather poor, it cannot effectively prevent the adhesion between the rubbing surfaces. Moreover, water can cause stress corrosion and crack growth, decreasing mechanical strength of the ceramic [12]. In this test, the wear rate increase of Si_3N_4 ceramic in water lubricated conditions may be attributed to the following factor. Water has strong penetrability, it can easily infiltrate into the preexisting surface flaws or microcracks produced in the rubbing process, accelerating the growth of the microcracks by stress corrosion. When the ceramic surface is subjected to repeated shear and compressive stresses, the microcrack growth and stress corrosion become more severe, resulting in microfracture or catastrophic failure of the ceramic. So microfracture wear of the ceramic occurs more frequently in water lubricated conditions. Although the adhesion between the rubbing surfaces is prevented to some extent the wear rate of the ceramic is increased. The microfracture wear process caused by water can be schematically described as Fig. 11. Considering the poor thermal shock resistance of the ceramic, it is possible that rapid cooling action of water (because of its high heat-adsorption capacity) results in more microcracks, especially at higher sliding speed, which also increases the microfracture wear of the ceramic.

In addition to the microfracture wear mechanism, chemical wear of the ceramic also occurs in water-lubricated conditions. SEM examinations of the worn Si_3N_4 surfaces suggest that an amorphous layer was formed on the ceramic surface, see Fig. 12, which could be the result of corrosion by water. In order to reveal the formation mechanism of the amorphous layer, the worn ceramic surface and the original ceramic surface were examined by AES. The results are shown in Fig. 13 and Table 2, respectively, from which it can be found that the atom concentration of nitrogen element decreased and that of oxygen element increased on the worn ceramic surface compared with the original

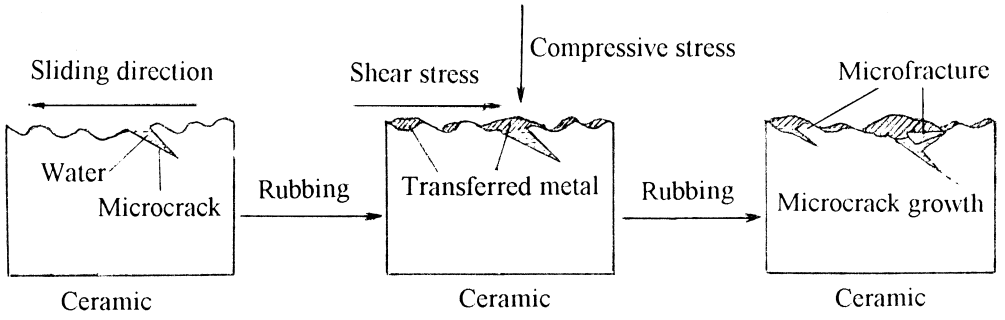

Fig. 11. Microfracture process of the ceramic caused by water.

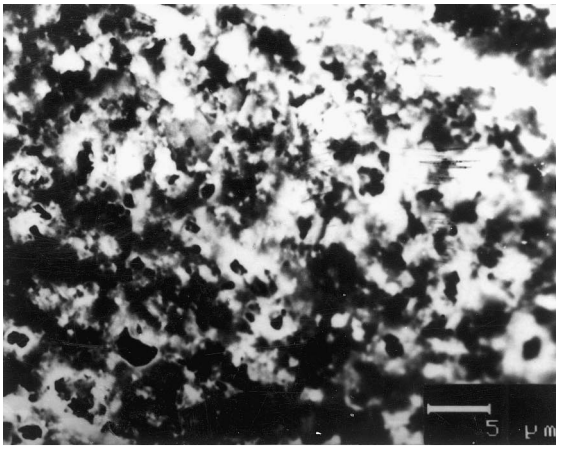

(a)

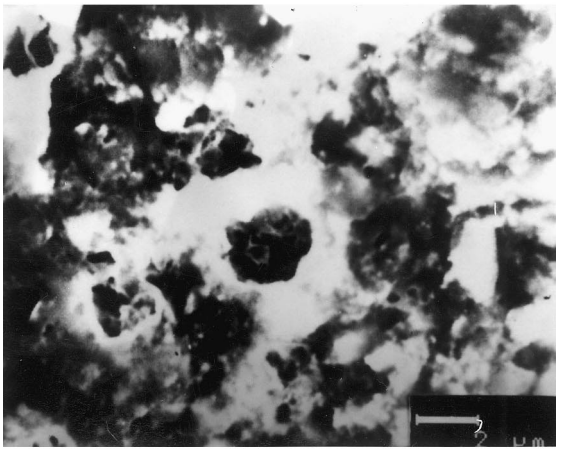

(b)

Fig. 12. SEM morphology of the amorphous layer formed on the worn ceramic surface.

surface. In addition, the peak of carbon element also decreased in the worn ceramic surface (in Fig. 13b), showing the decrease of atom concentration of carbon element. The XRD pattern of the worn ceramic surface (see Fig. 14) shows the existence of $FeSiO_3$ and SiO_2.

All these results indicate that the tribochemical reactions may occur in the water-lubricated conditions. Refs.

Table 2
Atom concentration (%) examined by AES

Elements	Original Si_3N_4 surface	Worn Si_3N_4 surface
N	23.7	4.9
O	23.1	42.2
Ti	4.8	5.1
Al	18.8	11.6
Fe	6.8	13.5
Si	17.1	16.8
Zr	5.7	5.9

[13–15] considered that Si_3N_4 can be oxidized by water in the rubbing process and then its oxides can dissolve in water to form silicic acid. In this paper, the possible tribochemical reactions were proposed as follows:

$$Si_3N_4 + 6H_2O \rightarrow 3SiO_2 + 4NH_3$$

$$SiO_2 + H_2O \rightarrow Si(OH)_4$$

$$SiO_2 \text{ or } Si(OH)_4 + FeO \rightarrow FeSiO_3$$

So the amorphous layer on the worn ceramic surface may be mainly composed of $FeSiO_3$ and SiO_2. The holes in the microstructure may be formed by the corrosion of water to the ceramic. The corrosion firstly occurs between Si_3N_4 grains and the glassy phase of the ceramic because more SiO_2 may be produced on the Si_3N_4 grain surface and it is an active area for chemical reactions, then the Si_3N_4 grains can be easily pulled out, thus a lot of microholes are produced. The worn ceramic surface becomes porous, its microstructure is destroyed and its strength is decreased. In this way, water also gives rise to the ceramic wear increase. The tribochemical products, on the one hand, prevent the rubbing surfaces from adhesion, reducing the friction coefficient; on the other hand, they bring about the chemical wear of the ceramic, increasing the wear rate.

In water-lubricated conditions, the adhesive wear also occurs because of the poor lubricity of water. The tribochemical products formed on the worn ceramic surface prevent the adhesion to some extent, so the friction coefficient is reduced. In addition to the adhesive wear,

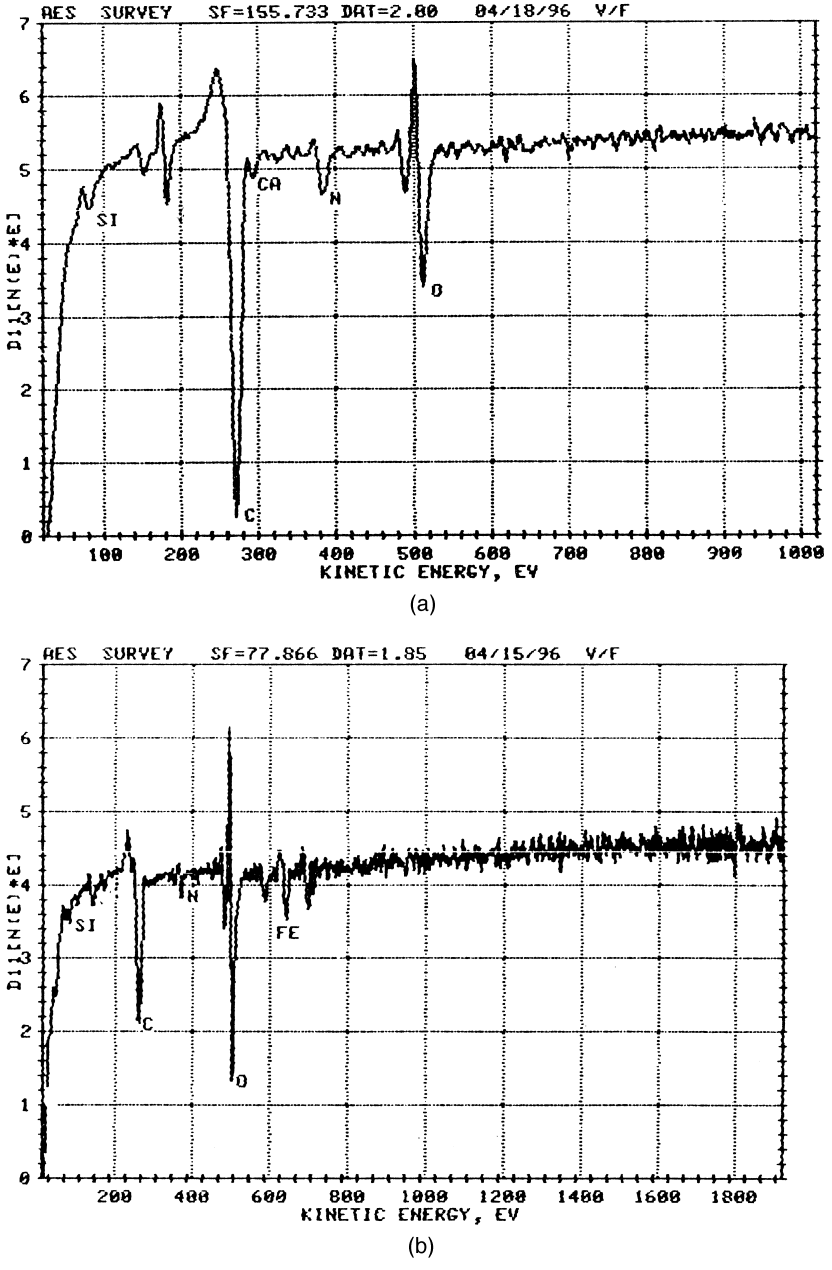

Fig. 13. AES spectrum of the ceramic surface (a) original surface (b) worn surface water-lubricated.

the wear of the ceramic in this condition is also attributed to microfracture wear and chemical wear.

4. Conclusion

From the above test results and surface examinations, the following conclusions can be summarized.

1. In Si_3N_4 ceramic/stainless steel sliding contacts, the wear of the ceramic is mainly caused by the adhesion-peeling off process. Stainless steel firstly transfers on the ceramic surface, then the transferred stainless steel flats will be subjected to repeated shear and compressive stresses until they are peeled off the rubbing ceramic surface. When the transferred stainless steel flats are peeled off the ceramic surface, some ceramic fragments or grains are also pulled out and taken away. Higher load brings about more severe adhesive wear and microfracture wear of the ceramic.
2. With load and speed increasing, the friction heat of the rubbing surfaces increases rapidly, which will accelerate adhesion between the rubbing surfaces, increasing adhesion wear and

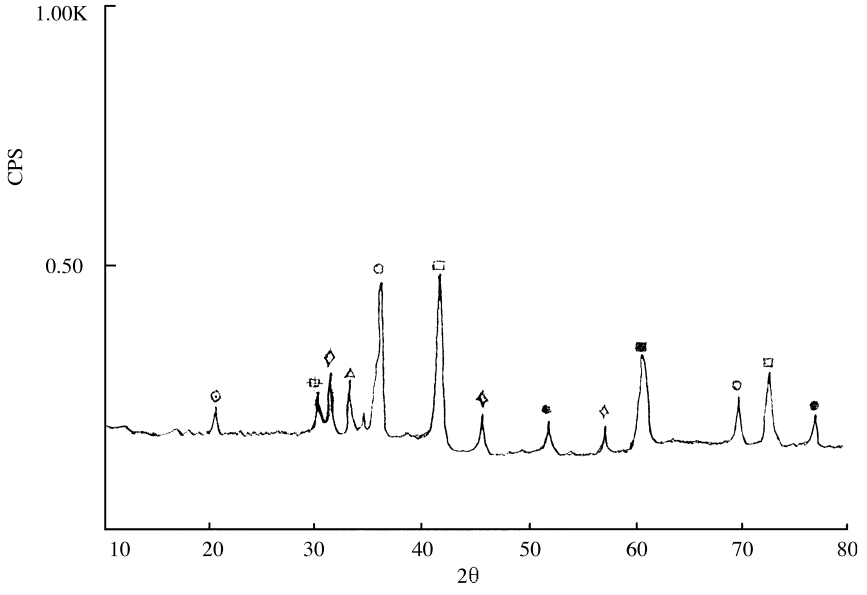

Fig. 14. XRD pattern of the worn ceramic surface. ○-Si_3N_4 □-TiC ◇-Al_2O_3 ⊞-$FeSiO_3$ ⊙-SiO_2 ●-Ni ■-TiN △-Fe_2O_3.

microfracture, so the wear of the ceramic increases with load and speed.

3. In water-lubricated conditions, the friction coefficient is slightly reduced because water prevents the adhesion of the rubbing surfaces to some extent, but water can accelerate the microcrack growth, causing severe microfracture wear. In addition, it also brings about chemical wear of the ceramic.
4. The test results show that water or even water-based cutting fluids may be unsuitable for lubricating Si_3N_4-based ceramic cutting tools.

Acknowledgements

The authors would like to thank National Natural Sciences Foundation of China and Laboratory of Solid Lubrication, Lanzhou Institute of Chemical Physics, Chinese Academy of Sciences, for their financial support to this project.

References

[1] T.N. Blackman, Foundryman 3 (1990) 17–24.
[2] J. Aucote, S.R. Foster, Mater. Sci. Technol. 2 (1986) 700–708.
[3] N. Richards, D. Aspinwall, Inter. J. Mach. Tools Manufact. 29 (1989) 575–588.
[4] S.K. Samanta, K. Subramanian, A. Exis, US Patent No. 4323325.
[5] J. Vleugels, T. Laoui, K. Vercammen, J.P. Celis, O. Van Der Biest, Materials Science and Engineering A187 (1994) 177–182.
[6] E.K. Asibu, J. Manuf. Systems 9 (1990) 159–168.
[7] M.K. Brun, M. Lee, Ceram. Eng. Sci. Proc. 4 (1983) 646–662.
[8] R. Rigaut, Y.M. Chen, J. Saint Chely, Lub. Eng. 50 (1994) 485–489.
[9] G. Brant, A. Gerendas, M. Mikus, J. Euro. Ceram. Soc. 6 (1990) 273–290.
[10] B.M. Kramer, N.P. Suh, J. Eng. Ind. 102 (1980) 303–309.
[11] B.M. Kramer, P.K. Judd, J. Vac. Sci. Technol A3 (1985) 2439–2444.
[12] T.A. Michalske, S.W. Freiman, J. Am. Ceram. Soc. 66 (1983) 284–288.
[13] T.E. Fischer, H. Tomizawa, in: K.C. Ludema (Ed.), Proc. Int. Conf. on Wear of Materials, ASME, 1985, pp. 22–32.
[14] H. Tomizawa, T.E. Fischer, ASLE Transactions 30 (1987) 41–46.
[15] S. Kitaoka, T. Tsuji, T. Katoh, J. Am. Ceram. Soc. 77 (1994) 580–588.